**Atmospheric
Chemistry
and Physics**

Determination of land surface heat fluxes over heterogeneous landscape of the Tibetan Plateau by using the MODIS and in situ data

Y. Ma[1], L. Zhong[1,2], B. Wang[1,3], W. Ma[4], X. Chen[1,2,3], and M. Li[4]

[1]Key Laboratory of Tibetan Environment Changes and Land Surface Processes, Institute of Tibetan Plateau Research, Chinese Academy of Sciences, Beijing, China
[2]International Institute for Geo-Information Science and Earth Observation, Enschede, The Netherlands
[3]Graduate University of Chinese Academy of Sciences, Beijing 100049, China
[4]Cold and Arid Regions Environmental and Engineering Research Institute, Chinese Academy of Sciences, Lanzhou 730000, China

Abstract. In this study, a parameterization methodology based on MODIS (Moderate Resolution Imaging Spectroradiometer) and in situ data is proposed and tested for deriving the regional surface reflectance, surface temperature, net radiation flux, soil heat flux, sensible heat flux and latent heat flux over heterogeneous landscape. As a case study, the methodology was applied to the Tibetan Plateau area. Four images of MODIS data (30 January 2007, 15 April 2007, 1 August 2007 and 25 October 2007) were used in this study for the comparison among winter, spring, summer and autumn. The derived results were also validated by using the "ground truth" measured in the stations of the Tibetan Observation and Research Platform (TORP). The results show that the derived surface variables (surface reflectance and surface temperature) and surface heat fluxes (net radiation flux, soil heat flux, sensible heat flux and latent heat flux) in four different seasons over the Tibetan Plateau area are in good accordance with the land surface status. These parameters show a wide range due to the strong contrast of surface features over the Tibetan Plateau. Also, the estimated land surface variables and surface heat fluxes are in good agreement with the ground measurements, and all their absolute percent difference (APD) is less than 10 % in the validation sites. It is therefore concluded that the proposed methodology is successful for the retrieval of land surface variables and surface heat fluxes using the MODIS and in situ data over the Tibetan Plateau area. The shortage and further improvement of the methodology were also discussed.

1 Introduction

The Tibetan Plateau contains the world's highest elevation (average elevation about 4000 m) relief features, some reaching into the mid-troposphere. It represents an extensive mass extending from subtropical to middle latitudes and is spanning over 25 degrees of longitude. Figure 1 shows the geographic location and topographic characteristics of the TP. Because of its topographic character, the plateau surface absorbs a large amount of solar radiation energy, and undergoes dramatic seasonal changes of surface heat and water fluxes (e.g., Ye and Gao, 1979; Ye, 1981; Yanai et al., 1992; Ye and Wu, 1998; Ma et al., 2002a; Ma and Tsukamoto, 2002; Hsu and Liu, 2003; Yang et al., 2004; Ma et al., 2006; Sato and Kimura, 2007; Ma et al., 2008; Cui and Graf, 2009; Zhong et al., 2010). In order to understand the effect of the Tibetan Plateau on the climatic change over China, east Asia and even the global, one has to get the regional distribution of surface heat fluxes over whole Tibetan Plateau.

Remote sensing from satellites however offers the possibility to derive regional distribution of surface heat fluxes over heterogeneous land surface of the Tibetan Plateau in combination with sparse field experimental stations. The

Correspondence to: Y. M. Ma
(ymma@itpcas.ac.cn)
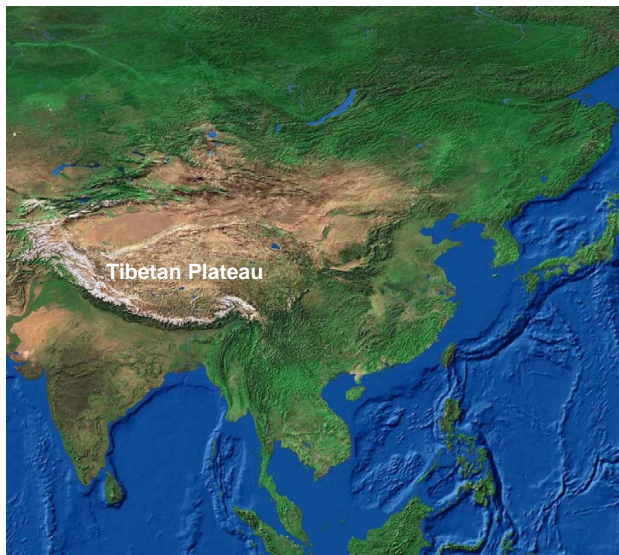
Fig. 1. The location and landscape of the Tibetan Plateau.

regional distributions of surface heat flux(net radiation flux, soil heat flux, sensible heat flux and latent heat flux) have already been gotten by some researchers over the Tibetan Plateau area, but the results were only in meso-scale area till now (e.g. Ma et al., 2003, 2006, 2009). The objective of this study is to explore the feasibility of up-scaling the point land surface variables (surface reflectance and surface temperature) and surface heat fluxes to yield whole Plateau spatial distributions with the aid of MODIS and in situ data.

2 Theory and scheme

The general concept of the methodology is shown in a diagram (Fig. 2). The surface reflectance for short-wave radiation $r_0(x,y)$ is retrieved from MODIS data with the atmospheric correction, using land surface and aerological observation data (Zhong, 2007). The land surface temperature $T_{sfc}(x,y)$ is also derived from MODIS data, land surface and aerological observation data (Zhong et al., 2010). The radiative transfer model MODTRAN (Berk et al., 1989) compute the downward short-wave and long-wave radiation at the surface (Ma and Tsukamoto, 2002). With these results the regional surface net radiation flux $R_n(x,y)$ is determined. The regional soil heat flux $G_0(x,y)$ is estimated from $R_n(x,y)$ and field observations over the Tibetan Plateau. The regional sensible heat flux $H(x,y)$ is estimated from $T_{sfc}(x,y)$, surface and aerological data with the aid of so-called "tile approach" (Ma et al., 2010), and the regional latent heat flux $\lambda E(x,y)$ can be derived as the residual of the energy budget theorem for land surface.

2.1 Net radiation flux

The regional net radiation flux can be derived from

$$R_n(x,y) = (1 - r_0(x,y)) \cdot K_\downarrow(x,y) + L_\downarrow(x,y) - \varepsilon_0(x,y)\sigma T_{sfc}^4(x,y) \quad (1)$$

where $r_0(x,y)$ and $T_{sfc}(x,y)$ are surface reflectance and surface temperature respectively. They can be derived from MODIS data with the atmospheric correction, using land surface and aerological observation data (Zhong, 2007; Zhong et al., 2010). Surface emissivity of $\varepsilon_0(x,y)$ in Eq. (1) is a function of the vegetation coverage $P_v(x,y)$. It can be derived from the model of Valor and Caselles (1996) i.e.

$$\varepsilon_0(x,y) = \varepsilon_v(x,y)P_v(x,y) + \varepsilon_g(x,y)(1 - P_v(x,y)) + 4 \\ <d\varepsilon>(1 - P_v(x,y))P_v(x,y) \quad (2)$$

where $\varepsilon_v(x,y) = 0.985\ (\pm 0.007)$ and $\varepsilon_g(x,y) = 0.960\ (\pm 0.010)$ are surface emissivity for full vegetation and bare soil respectively, $<d\varepsilon> = 0.015(\pm 0.008)$ is the error, and vegetation coverage (Carlson and Ripley, 1997)

$$P_v(x,y) = \left[\frac{NDVI(x,y) - NDVI_{min}}{NDVI_{max} - NDVI_{min}}\right]^2 \quad (3)$$

where $NDVI_{min}$ and $NDVI_{max}$ are the NDVI values for bare soil and full vegetation, respectively.

The incoming long-wave radiation flux $L_\downarrow(x,y)$ and incoming short-wave radiation flux $K_\downarrow(x,y)$ in Eq. (1) can be calculated from radiative transfer model MODTRAN directly (Ma and Tsukamoto, 2002).

2.2 Soil heat flux

The regional surface soil heat flux $G_0(x,y)$ can be determined by (Choudhury and Monteith, 1988)

$$G_0(x,y) = \rho_s c_s[(T_{sfc}(x,y) - T_s(x,y)]/r_{sh}(x,y) \quad (4)$$

where ρ_s is soil dry bulk density, c_s is soil specific heat, $T_s(x,y)$ stands for soil temperature at a determined depth, $r_{sh}(x,y)$ represents soil heat transfer resistance.

$G_0(x,y)$can not directly be mapped from satellite measurements through Eq. (4). The difficulty is to derive $r_{sh}(x,y)$ and $T_s(x,y)$ (Bastiaanssen, 1995; Wang et al., 1995; Ma and Tsukamoto, 2002; Ma et al., 2002b; Ma et al., 2003; Ma et al., 2006; Ma et al., 2007; Gao et al., 2010). To calculate the values of $G_0(x,y)$ solely from remote sensed data requires that it is to be made proportional to another term in the energy balance equation. A good candidate is $R_n(x,y)$ (Jackson et al., 1985; Choudhury et al., 1987; Kustas and Daughtry, 1990; Bastiaanssen, 1995; Ma and Tsukamoto, 2002; Ma et al., 2003, 2006; Gao et al., 2010). Based on the in situ data observed in the TP area, Ma et al. (2002b) proposed an equation to derive regional soil heat flux $G_0(x,y)$ from regional
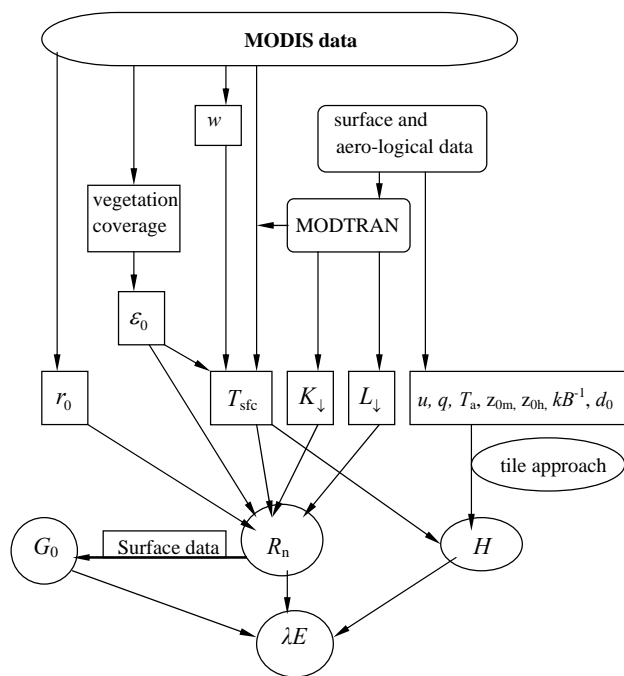
Fig. 2. The diagram of parameterization procedure to determine surface reflectance, surface temperature, net radiation flux, soil heat flux, sensible heat flux and latent heat flux by combining MODIS data with field observations.

net radiation flux $R_n(x,y)$ based the in situ data over the Tibetan Plateau. It is

$$G_0(x,y) = 0.35462(\pm 0.00235) R_n(x,y) - 47.79008(\pm 0.70005) \quad (5)$$

Eq. (5) will be used to determine the regional distribution of soil heat flux in the TP area in this study.

2.3 Sensible heat flux

The sensible heat flux H can be estimated with a bulk transfer equation written in the form (Montheith, 1973)

$$H = \rho\, c_p \frac{T_0 - T_a}{r_{ah}} \quad (6)$$

where r_{ah} is aerodynamic resistance for heat transfer between land surface and reference height, T_0 is the surface temperature, T_a is the air temperature at the reference height, ρ is the air density, and c_p is the air specific heat at constant pressure.

In order to determine the regional distribution of sensible heat flux $H(x,y)$ over the Tibetan Plateau, the Tile approach (Ma et al., 2010) will be used here. In the Tile approach, the reference height z_{ref} is taken within Surface Layer (SL). Then, using the satellite measurements at the surface and the SL observations on a "tile" at and below the reference height (e.g. 20 m), the heat fluxes over a heterogeneous landscape can be estimated. Firstly, surface reflectance r_0, surface temperature T_{sfc} vegetation coverage P_v and surface emissivity ε_0 etc. at the surface are derived from satellite

measurements. Secondly, SL observations on a *tile*: wind speed u, air temperature T_a and specific humidity q at the reference height are carried out. Zero-plane displacement d_0, aerodynamic roughness length z_{0m} and thermodynamic roughness length z_{0h}, the excess resistance for heat transportation kB^{-1} and the like in SL below the reference height over the i−tile are used to estimate the sensible heat flux H (Fig. 2).

Hence, in mathematical terms:

$$H_1(x,y) = \rho c_p \frac{[T_0(x,y) - T_{a1}]}{r_{ah1}},$$

$$H_2(x,y) = \rho c_p \frac{[T_0(x,y) - T_{a2}]}{r_{ah2}}, \quad (7)$$

$$\dots \dots$$

$$H_n(x,y) = \rho c_p \frac{[T_0(x,y) - T_{an}]}{r_{ahn}}$$

Therefore, H over whole Tibetan Plateau area can be derived from:

$$H(x,y) = \sum_{i=1}^{n} a(i) H_i(x,y) \quad (8)$$

where $a(i)$ is the fractional ratio of each "tile" for the Tibetan Plateau, and it can be determined form the satellite images. $H_1(x,y)$, $H_2(x,y) \dots$, and $H_n(x,y)$ are sensible heat flux on each "tile", T_{a1}, $T_{a2}\dots$, and T_{a2} are air temperature at the reference height on each "tile", $r_{ah1}, r_{ah2} \dots$, and r_{ahn} are aerodynamic resistance for heat transfer between land surface and reference height on each "tile". $r_{ah1}, r_{ah2} \dots$, and r_{ahn} can be determined from the eddy diffusion coefficients for heat transport between the land surface and the reference height (Ma et al., 2010).

2.4 Latent heat flux

The regional latent heat flux $\lambda E(x,y)$ can be derived as the residual of the energy budget theorem for land surface based on the condition of zero horizontal advection, i.e.,

$$\lambda E(x,y) = R_n(x,y) - H(x,y) - G_0(x,y) \quad (9)$$

3 Cases study and validation

Four images of MODIS data (30 January 2007, 15 April 2007, 1 August 2007 and 25 October 2007) will be used in this study for the comparison among winter, spring, summer and autumn.

Figure 3 shows the distribution maps of surface reflectance and surface temperature over the Tibetan Plateau area. Using Eqs. (1) and (9), the distributions of soil heat flux and latent heat flux are shown in Fig. 4. The distribution maps of surface reflectance, surface temperature, soil heat flux and latent heat flux are based on 2823×1441

Table 1. Comparison of the derived surface reflectance, surface temperature, net radiation flux and soil heat flux(Cal.) versus the values measured (Meas.) at the Tibetan Plateau with absolute percent difference (APD).

January	$r_{0(-)}$			T_s (°C)			R_n (Wm^{-2})			G_0(Wm^{-2})		
Sites	Cal.	Meas.	APD	Cal.	Meas.	APD	Cal.	Meas.	APD	Cal.	Meas.	APD
Haibei	0.21	0.22	4.5 %	20.0	19.0	5.3 %	347	331	4.8 %	64	59	8.5 %
Maqu	0.22	0.23	4.3 %	19.0	18.0	5.6 %	383	353	8.5 %	93	85	9.4 %
D105	0.26	0.25	4.0 %	11.0	10.0	10.0 %	351	321	9.3 %	99	91	8.8 %
Amdo	0.21	0.23	8.7 %	16.0	15.0	6.7 %	382	354	7.9 %	96	92	4.3 %
NPAM	0.18	0.19	5.3 %	15.0	14.0	7.1 %	404	413	2.2 %	68	62	9.7 %
BJ	0.25	0.27	7.4 %	2.0	2.0	0.0 %	311	285	9.1 %	94	87	8.0 %
NAMOR	0.43	0.41	4.9 %	−2.0	−2.0	0.0 %	358	343	4.4 %	72	66	9.1 %
QOMS	0.28	0.29	3.4 %	6.0	6.0	0.0 %	367	337	8.9v%	103	94	9.6 %
SETS	0.18	0.19	5.3 %	18.0	19.0	5.3 %	436	457	4.6 %	54	50	8.0 %

April	$r_{0(-)}$			T_s (°C)			R_n (Wm^{-2})			G_0(Wm^{-2})		
Sites	Cal.	Meas.	APD	Cal.	Meas.	APD	Cal.	Meas.	APD	Cal.	Meas.	APD
Haibei	0.24	0.22	9.1 %	14.0	15.0	6.7 %	603	621	2.9 %	86	79	8.9 %
Maqu	0.24	0.23	4.3 %	21.0	23.0	8.7 %	449	431	4.2 %	90	82	9.7 %
D105	0.25	0.24	4.2 %	13.0	12.0	8.3 %	352	323	9.0 %	86	80	7.5 %
Amdo	0.23	0.21	9.5 %	29.0	27.0	7.4 %	410	388	5.7 %	89	83	7.2 %
NPAM	0.19	0.18	5.6 %	35.0	34.0	2.9 %	606	644	5.9 %	91	85	7.1 %
BJ	0.23	0.22	4.5 %	29.0	27.0	7.4 %	441	432	2.1 %	108	101	6.9 %
NAMOR	0.22	0.21	4.8 %	17.0	16.0	6.3 %	522	515	1.4 %	96	92	4.3 %
QOMS	0.27	0.26	3.8 %	20.0	21.0	4.8 %	475	466	1.9 %	139	133	4.5 %
SETS	0.19	0.20	5.0 %	29.0	32.0	9.4 %	611	648	5.7 %	94	87	8.0 %

August	$r_{0(-)}$			T_s (°C)			R_n (Wm^{-2})			G_0(Wm^{-2})		
Sites	Cal.	Meas.	APD	Cal.	Meas.	APD	Cal.	Meas.	APD	Cal.	Meas.	APD
Haibei	0.23	0.22	4.5 %	21.0	22.0	4.5 %	358	350	2.3 %	88	82	7.3 %
Maqu	0.18	0.19	5.3 %	24.0	25.0	4.0 %	694	639	8.6 %	138	126	9.5 %
D105	0.22	–	–	19.0	–	–	633	–	–	110	101	8.9 %
Amdo	0.19	–	–	20.0	–	–	686	–	–	126	–	–
NPAM	0.14	0.13	7.7 %	20.0	19.0	5.3 %	737	780	5.5 %	115	108	6.5 %
BJ	0.15	0.16	6.3 %	24.0	23.0	4.3 %	702	665	5.6 %	142	135	5.1 %
NAMOR	0.18	0.19	5.3 %	27.0	29.0	6.9 %	715	656	9.0 %	148	139	6.5 %
QOMS	0.18	0.17	5.9 %	21.0	20.0	5.0 %	700	678	3.2 %	180	169	6.5 %
SETS	0.18	0.17	5.9 %	25.0	27.0	7.4 %	751	724	3.7 %	92	87	5.7 %

October	$r_{0(-)}$			T_s (°C)			R_n (Wm^{-2})			G_0(Wm^{-2})		
Sites	Cal.	Meas.	APD	Cal.	Meas.	APD	Cal.	Meas.	APD	Cal.	Meas.	APD
Haibei	0.16	0.17	5.9 %	3.0	3.0	0.0 %	478	456	4.8 %	82	77	6.5 %
Maqu	0.18	0.19	5.3 %	24.0	26.0	7.7 %	476	434	9.7 %	93	86	8.1 %
D105	0.23	0.21	9.5 %	15.0	16.0	6.3 %	465	432	7.6 %	100	91	9.9 %
Amdo	0.21	–	–	19.0	21.0	9.5 %	475	–	–	107	116	7.8 %
NPAM	0.17	0.16	6.3 %	14.0	13.0	7.7 %	516	527	2.1 %	73	67	9.0 %
BJ	0.21	0.20	5.0 %	20.0	21.0	4.8 %	443	406	9.1 %	126	117	7.7 %
NAMOR	0.33	–	–	−1.0	−1.0	0.0 %	479	–	–	93	85	9.4 %
QOMS	0.23	0.25	8.0 %	17.0	16.0	6.3 %	448	424	4.7 %	132	136	2.9 %
SETS	0.16	0.17	5.9 %	22.0	24.0	8.3 %	472	–	–	83	76	9.2 %

Table 2. Comparison of the derived sensible heat flux and latent heat flux (Cal.) versus the values measured (Meas.) at the Tibetan Plateau with absolute percent difference (APD).

	January: $H(\mathrm{Wm}^{-2})\ \lambda E(\mathrm{Wm}^{-2})$						April: $H(\mathrm{Wm}^{-2})\ \lambda E\,(\mathrm{Wm}^{-2})$					
Sites	Cal.	Meas.	APD	Cal.	Meas.	APD	Cal.	Meas.	APD	Cal.	Meas.	APD
Haibei	197	211	6.6 %	138	146	5.5 %	400	381	5.0 %	264	268	1.5 %
Maqu	155	142	9.2 %	36	33	9.1 %	286	296	3.4 %	156	143	9.1 %
D105	281	267	5.2 %	20	19	5.3 %	283	289	2.1 %	153	148	3.4 %
Amdo	267	275	2.9 %	16	15	6.7 %	298	307	3.0 %	142	135	5.2 %
NPAM	281	264	6.4 %	28	30	6.7 %	378	395	4.3 %	124	114	8.8 %
BJ	176	192	8.3 %	12	11	9.1 %	342	355	3.7 %	119	127	6.3 %
NAMOR	267	270	1.1 %	17	16	6.3 %	172	169	1.8 %	176	181	2.8 %
QOMS	225	244	7.8 %	46	42	9.5 %	142	148	4.1 %	37	40	7.5 %
SETS	267	252	6.0 %	19	18	5.6 %	139	144	3.5 %	145	141	2.8 %
	August: $H(\mathrm{Wm}^{-2})\ \lambda E(\mathrm{Wm}^{-2})$						October: $H(\mathrm{Wm}^{-2})\ \lambda E\,(\mathrm{Wm}^{-2})$					
Sites	Cal.	Meas.	APD	Cal.	Meas.	APD	Cal.	Meas.	APD	Cal.	Meas.	APD
Haibei	120	111	8.1 %-	279	264	5.7 %	235	253	7.1 %	97	93	4.3 %
Maqu	158	–	–	560	–	–	95	101	5.9 %	101	92	9.8 %
D105	174	–	–	349	–	–	342	347	1.4 %	82	78	5.1 %
Amdo	162	–	–	398	–	–	137	131	4.6 %	90	86	4.4 %
NPAM	160	176	9.1 %	575	603	4.6 %	398	420	5.5 %	170	158	7.6 %
BJ	159	173	8.8 %	411	398	3.3 %	275	294	6.5 %	42	39	7.7 %
NAMOR	129	141	8.5 %	468	506	7.5 %	102	96	6.3 %	57	54	5.6 %
QOMS	77	82	6.1 %	220	201	9.5 %	137	140	2.1 %	26	24	8.3 %
SETS	106	112	5.4 %	469	482	2.7 %	132	136	2.9 %	151	141	7.1 %

pixels with a size of $1 \times 1\,\mathrm{km}^2$. The derived surface reflectance, surface temperature, net radiation flux, soil heat flux, sensible heat flux and latent heat flux can be validated by the field measurements. In situ data observed in nine stations of Haibei (37.62° N, 101.30° E; elevation: 3220 m; land-cover: grassy marshland), Maqu (33.89° N, 102.14° E; elevation: 3423 m; land-cover: grassy marshland), D105 (33.06° N, 91.94° E; elevation: 5039 m; land-cover: sparseness meadow), Amdo (32.14° N, 91.37° E; elevation: 4695 m; land-cover: grassy marshland), NPAM (31.93° N, 91.71° E; elevation: 4620 m; land-cover: grassy marshland), BJ (31.37° N, 91.90° E; elevation: 4509 m; land-cover: sparseness meadow), NAMOR(Nam Co Station for Multisphere Observation and Research, Chinese Academy of Sciences; 30.46° N, 90.59° E; elevation: 4730 m; land-cover: grassy marshland), QOMS(Qomolangma Station for Atmospheric and Environmental Observation and Research, Chinese Academy of Sciences; 28.21° N, 86.56° E; elevation: 4276 m; land-cover: sparse grass-Gobi) and SETS(Southeast Tibet Station for Alpine Environment Observation and Research, Chinese Academy of Sciences; 29.77° N, 94.73° E; elevation: 3326 m; land-cover: grass land) in the Tibetan Observation and Research Platform (TORP, Ma et al., 2008) are used for the validation. In Tables 1, 2 and Fig. 5, the derived results are validated against the measured values in the stations. Since it is a little difficult to determine the loca-

tions of the four stations, the values of 5×5 pixel rectangle, surrounding the determined Universal Transfer Macerator (UTM) coordinate, are compared with the in situ data. The absolute percent difference (APD) was quantitatively measures the difference between the derived results ($H_{\mathrm{derived(i)}}$) and measured value ($H_{\mathrm{measured(i)}}$) here, and

$$\mathrm{APD} = \frac{\left| H_{\mathrm{derived(i)}} - H_{\mathrm{measured(i)}} \right|}{H_{\mathrm{measured(i)}}} \tag{10}$$

The results show that: (1) The derived surface reflectance (r_0), surface temperature (T_{sfc}), net radiation heat flux (R_n), soil heat flux (G_0), sensible heat flux (H) and latent heat flux (λE) for the Tibetan Plateau area are in good accordance with the land surface status, and they show a wide range due to the strong contrast of surface features over there (Figs. 1, 3 and 4). Surface reflectance is from 0.00 to 0.50 in January (some of the surface reflectance with value large than 0.50 indicating cloud-covering), it is from 0.00 to 0.45 in April (some of the surface reflectance with value large than 0.45 indicating cloud-covering), it is from 0.00 to 0.45 in August (some of the surface reflectance with value large than 0.45 indicating cloud-covering), it is from 0.00 to 0.50 in October (some of the surface reflectance with value large than 0.50 indicating cloud-covering) (Fig. 3); Surface temperature range from −30 °C to 20 °C in January, it range from −40 °C to 36 °C in April, it is from −20 °C to 55 °C in August, and it is from −30 °C to 30 °C in October (the blue parts
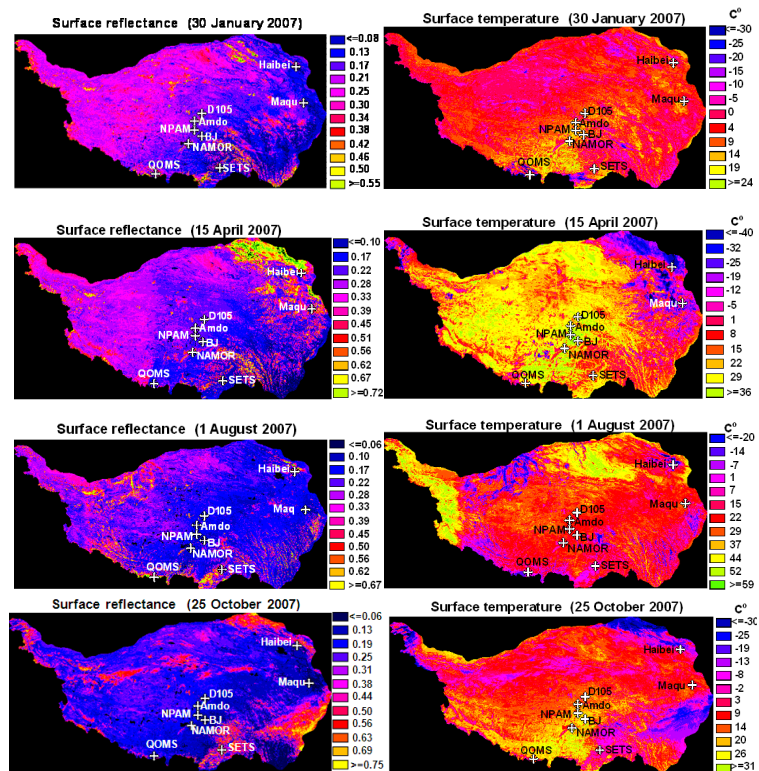
Fig. 3. The distribution maps of surface reflectance and surface temperature over the Tibetan Plateau area.
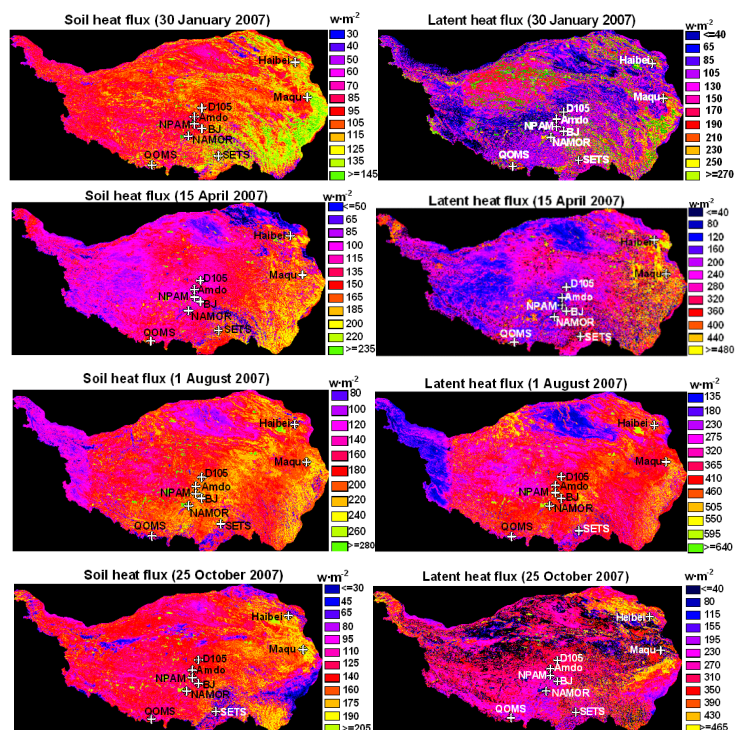
Fig. 4. The distribution maps of surface soil heat flux and latent heat flux over the Tibetan Plateau area.
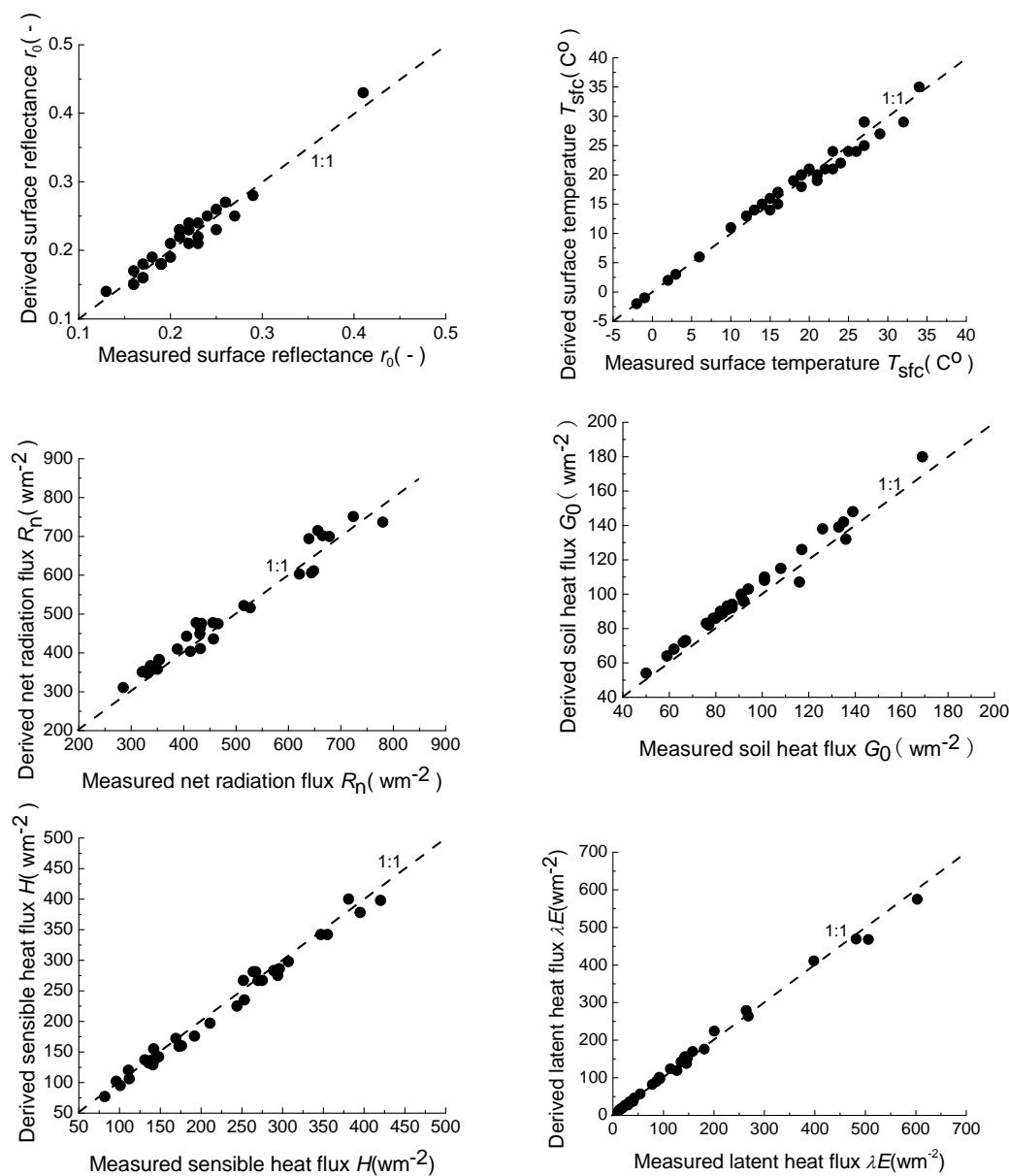
Fig. 5. Comparison of derived results with field measurements for the surface reflectance, surface temperature, net radiation flux, soil heat flux, sensible heat flux and latent heat flux over the Tibetan Plateau area, together with a 1:1 line.

in the distribution maps indicating cloud-covering) (Fig. 3); R_n change from 115 to 550 W m^{-2} in January, it varies from 170 to 700 W m^{-2} in April, it is from 200 to 920 W m^{-2} in August, and varies from 100 to 700 W m^{-2} in October; G_0 varies from 30 to 140 W m^{-2} in January, it changes from 50 to 220 W m^{-2} in April, it is from 80 to 275 W m^{-2} in August, and varies from 80 to 260 W m^{-2} in October (Fig. 4); H change from 0 to 280 W m^{-2} in January, it varies from 0 to 300 W m^{-2} in April, it is from 0 to 200 W m^{-2} in August, and varies from 0 to 480 W m^{-2} in October; λE is from 40 to 250 W m^{-2} in January, it varies from 40 to 400 W m^{-2}

in April, it change from 135 to 640 W m^{-2} in August, and varies from 40 to 450 W m^{-2} in October (Fig. 4); (2) the derived surface reflectance, surface temperature, net radiation flux, soil heat flux, sensible heat flux and latent heat flux over the Tibetan Plateau area are very close to the field measurements. The difference between the derived results and the field observation APD is less than 10 % (Tables 1, 2 and Fig. 5). The reason is that accurate surface reflectance and surface temperature were determined and the process of atmospheric boundary layer was considered in more detail in the determination of sensible heat flux in the procedure; and

(3) The mean net radiation flux over the TP area is increasing from January to April and August, then decreasing from October. They are $415 \, \mathrm{W \, m^{-2}}$, $487 \, \mathrm{W \, m^{-2}}$, $630 \, \mathrm{W \, m^{-2}}$ and $505 \, \mathrm{W \, m^{-2}}$; The mean surface soil heat flux over the TP area is increasing from January to April and August, then decreasing from October. They are $99 \, \mathrm{W \, m^{-2}}$, $125 \, \mathrm{W \, m^{-2}}$, $175 \, \mathrm{W \, m^{-2}}$ and $131 \, \mathrm{W \, m^{-2}}$; The mean sensible heat flux over the TP area is decreasing from January to April and August, then increasing from October. They are $190 \, \mathrm{W \, m^{-2}}$, $142 \, \mathrm{W \, m^{-2}}$, $114 \, \mathrm{W \, m^{-2}}$ and $192 \, \mathrm{W \, m^{-2}}$; The mean latent heat flux over the TP area is increasing from January to April and August, then decreasing from October. They are $141 \, \mathrm{W \, m^{-2}}$, $254 \, \mathrm{W \, m^{-2}}$, $350 \, \mathrm{W \, m^{-2}}$ and $278 \, \mathrm{W \, m^{-2}}$.

4 Concluding remarks

In this study, the regional distributions of surface reflectance, surface temperature, net radiation flux, soil heat flux sensible heat flux and latent heat flux over heterogeneous landscape of the Tibetan Plateau are derived with the aid of MODIS and the in situ data. Compared with the field measurements, the proposed methodology has been proved to be a better approach to getting related land surface heat fluxes over heterogeneous landscape. It forms a sound basis to study the exchange processes of heat and water on heterogeneous land surface.

Regionalization the net radiation heat flux, soil heat flux, sensible heat flux and latent heat flux over heterogeneous landscape is not an easy issue. The parameterization methodology presented in this research is still in developing stage due to only a single set of values at a specific time of specific day are used in this research. To reach more accurate regional land surface heat fluxes over the Tibetan Plateau area, more field observations, more accurate radiation transfer models to determine the surface reflectance and surface temperature, and another satellites such as GMS (Geo-stationary Meteorological Satellite), ATSR (Along Track Scanning Radiometer) and AVHRR (Advanced Very High-Resolution Radiometer) have to be used. These research works will be done in the next step.

References

Bastiaanssen, W. G. M.: Regionalization of surface fluxes and moisture indicators in composite terrain, PhD Thesis, Wageningen Agricultural University, 273 pp., 1995.

Berk, A., Bernstein, L. S., and Robertson, D.C.: MODTRAN: A moderate resolution model for LOTRAN 7. GL-TR-89-0122, 1989.

Carlson, T. N. and Ripley, D. A.: On the relation between NDVI, fractional vegetation cover, and leaf area index, Remote Sens. Environ., 62, 241-252.1997,

Choudhury, B. J. and Monteith, J. L.: A four-layer model for the heat budget of homogeneous land surfaces, Q. J. Roy. Meteor. Soc., 114, 373–398, 1988.

Choudhury, B. J., Idso, S. B., and Reginato, R. J.: Analysis of an empirical model for soil heat flux under a growing wheat crop for estimating evaporation by infrared-temperature based energy balance Eq., Agr. Forest. Meteorol., 39, 283–297, 1987.

Cui, X. and Graf, H.: Recent land cover changes on the Tibetan Plateau: a review, Climatic Change, 94, 47–61, 2009.

Gao, Z., Horton, R., and Liu, H.: Impact of wave phase difference between soil surface heat flux and soil surface temperature on soil surface energy balance closure, J. Geophysics Research, 115, D16112, doi:10.1029/2009JD013278, 2010.

Hsu, H. and Liu, X.: Relationship between the Tibetan Plateau heating and East Asian summer monsoon rainfall, Geophys. Res Lett., 30, D2066, doi:10.1029/2003GL017909, 2003.

Jackson, R. D., Pinter, J. R., and Reginato, R. J.: Net radiation calculated from remote multispectral and ground station meteorological data, Agr. Forest. Meteorol., 35, 153–164, 1985.

Kustas, W. P. and Daughtry, C. S. T.: Estimation of the soil heat flux/net radiation ratio from spectral data, Agr. Forest. Meteorol., 39, 205–223, 1990.

Ma, Weiqiang, Ma, Yaoming, Li, Maoshan, Hu, Zeyong, Zhong, Lei, Su, Zhongbo, Ishikawa, Hirohiko, and Wang, Jiemin: Estimating surface fluxes over the north Tibetan Plateau area with ASTER imagery, Hydrol. Earth Syst. Sci., 13, 57–67, doi:10.5194/hess-13-57-2009, 2009.

Ma, Y. and Tsukamoto, O.: Combining satellite remote sensing with field observations for land surface heat fluxes over inhomogeneous landscape, China Meteorological Press, Beijing, China, 2002.

Ma, Y., Tsukamoto, O., Wang, J., Ishkawa, H., and Tamagawa, I.: Analysis of aerodynamic and thermodynamic parameters over the grassy marshland surface of Tibetan Plateau, Prog. Nat. Sci., 12, 36–40, 2002a.

Ma, Y., Su, Z., Li, Z.-L., Koike, T., and Menenti, M.: Determination of regional net radiation and soil heat flux densities over heterogeneous landscape of the Tibetan Plateau, Hydrol. Process., 16, 2963–2971 2002b.

Ma, Y., Ishikawa, H., Menenti, M., Su, Z., Yao, T., Koike, T., and Yasynari, T.: Regionalization of surface fluxes over heterogeneous landscape of the Tibetan Plateau by using satellite remote sensing, J. Meteorol. Soc. Jpn., 81, 277–293, 2003.

Ma, Y., Zhong, L., Z. Su, Z., Ishikawa, H., Menenti, M., and Koike, T.: Determination of regional distributions and seasonal variations of land surface heat fluxes from Landsat-7 Ehanced Thematic Mapper data over the central Tibetan Plateau area, J. Geophys. Res.-Atmos., 111, D10305, doi:10.1029/2005JD006742, 2006.

Ma, Y., Song, M., Ishikawa, H., Yang, K., Koike, T., Jia, L., Menenti, M., and Su, Z.: Estimation of the regional evaporative fraction over the Tibetan Plateau area by using Landsat-7 ETM data and the field observations, J. Meteorol. Soc. Jpn., 85A, 295–309, 2007.

Ma, Y., Kang, S., Zhu, L., Xu, B., Tian, L., and Yao, T.: Tibetan Observation and Research Platform- Atmosphere–land interaction over a heterogeneous landscape, Bull. Amer. Meteor. Soc., 89, 1487–1492, 2008.

Ma, Y., Menenti, M., and Feddes, R.: Parameterization of heat fluxes at heterogeneous surfaces by integrating satellite measurements with surface layer and atmospheric boundary layer observations, Adv. Atmos. Sci., 27, 328–336, 2010.

Montheith, J. L.: Principles of Environmental Physics, Edward Aarnold, London, 241 pp., 1973.

Sato, T. and Kimura, F.: How does the Tibetan Plateau affect the transition of Indian monsoon rainfall? Mon. Weather Rev., 135, 2006–2015 2007,

Valor, E. and Caselles, V.: Mapping land surface emissivity from NDVI: application to European, African, and South American areas, Remote Sens. Environ., 57, 167–184, 1996,

Wang, J., Ma, Y., Menenti, M., Bastiaanssen, W., and Mistuta, Y.: The scaling-up of processes in the heterogeneous landscape of HEIFE with the aid of satellite remote sensing, J. Meteorol. Soc. Jpn., 73, 1235–1244, 1995.

Yanai, M., Li, C., and Song, Z.: Seasonal heating of the Tibetan Plateau and its effects on the evolution of the Asian summer monsoon, J. Meteorol. Soc. Jpn., 70, 319–351, 1992.

Yang, K., Koike, T., Ishikawa, H., and Ma, Y.: Analysis of the surface energy budget at a site of GAME/Tibet using a single-source model, J. Meteorol. Soc. Jpn., 82, 131–153, 2004.

Ye, D.: Some characteristics of the summer circulation over the Qinghai-Xizang (Tibet) Plateau and its neighborhood, B. Am. Meteorol. Soc., 62, 14–19, 1981.

Ye, D. and Gao, Y.: The Meteorology of the Qinghai-Xizang (Tibet) Plateau , 1–278, Science Press, Beijing, 1979 (in Chinese).

Ye, D. and Wu, G.: The role of the heat source of the Tibetan Plateau in the general circulation, Meteorol. Atmos. Phys., 67, 181– 198, 1998.

Zhong, L.: Measurement and satellite remote sensing of land surface characteristic parameters over the Tibetan Plateau area, PhD Thesis, Graduate University of Chinese Academy of Sciences, 124 pp., 2007.

Zhong, L., Ma, Y., Salama, Mhd.Suhyb, and Su, Z.: Assessment of vegetation dynamics and their response to variations in precipitation and temperature in the Tibetan Plateau, Climatic Change, doi:10.1007/s10584-009-9787-8, 2010.